JOURNAL OF GEOPHYSICAL RESEARCH, VOL. 115, D08105, doi:10.1029/2009JD012188, 2010

Impacts of future climate change on soil frost in the midwestern United States

Tushar Sinha[1] and Keith A. Cherkauer[2]

Received 8 April 2009; revised 3 December 2009; accepted 9 December 2009; published 23 April 2010.

[1] Historical observations indicate a shift toward shorter winters and increased average air temperatures in the midwestern United States. Furthermore, a rise in soil temperatures is likely to be enhanced under projections of increased air temperature; however, reduced snow cover during winter may lead to colder soil temperatures in the future. Cumulatively, these changes will affect cold season processes in the region. Therefore the impact of such changes on cold season processes were analyzed under two climate models (Geophysical Fluid Dynamics Laboratory version CM2.1.1 (GFDL) and UK Met Office Hadley Center Climate Model, version 3.1 (HadCM3)) and three scenarios (B1, A1B, and A2) by implementing the variable infiltration capacity land surface model from 1977 to 2099. Ensemble averages of the two models for the three scenarios indicated that both air temperature and precipitation would increase in the cold season (December–May), with the greatest increases projected under the A2 scenario by late in the 21st century (2070–2099). Also during this period, the median number of days when air temperature was below 0°C reduced in comparison to the base period (1977–2006) by 25, 35, and 38 days for the B1, A1B, and A2 scenarios, respectively. The number of freeze-thaw cycles increased in the south-central Wisconsin and the northern regions of Michigan by up to 3 cycles, while the duration of soil frost decreased by between 2 weeks and nearly 2 months during 2070–2099 with respect to the base period.

Citation: Sinha, T., and K. A. Cherkauer (2010), Impacts of future climate change on soil frost in the midwestern United States, *J. Geophys. Res.*, *115*, D08105, doi:10.1029/2009JD012188.

1. Introduction

[2] At global and regional scales, long-term changes in climate have been observed. In 2005, the World Meteorological Organization (WMO) reported a sharp increase in global average air temperatures, at a rate of 0.18°C per decade since 1976, with most of the warming attributed to the anthropogenic greenhouse gas (GHG) emissions (see http://www.wmo.ch/index-en.html, *Santer et al.* [1996], and *Lemke et al.* [2007]). Instrumental records since 1850 indicate that the earth has experienced the majority of its warmest years of near-surface air temperatures from 1995 to 2006 [*Intergovernmental Panel on Climate Change* (*IPCC*), 2007]. In the Northern Hemisphere, mean snow cover area has been significantly reduced, and spring snowmelt has been occurring earlier in the year from 1972 to 2000 [*Lemke et al.*, 2007]. *Lemke et al.* [2007] also indicated a decrease in the maximum area covered by seasonally frozen ground by about 7% in the Northern Hemisphere since the 1900. Furthermore, historical observations indicate increased annual air temperatures, reducing days with below freezing air temperature by up to two weeks, and shortening the duration of winters in the Great Lakes region since the early 1900s [*Kling et al.*, 2003]. In the Missouri River basin, where snow plays a dominant role in hydrology, increased air temperature has reduced spring melt peaks while winter flows have increased [*Lettenmaier et al.*, 1999]. These changes in winter air temperatures and precipitation are likely to affect the role of the cold season hydrological processes.

[3] Cold season processes including seasonal soil frost and snow accumulation are dominant in the hydrology of the midwestern United States. Melting snow or rainfall events over a frozen ground surface may result in increased runoff as soil ice impedes infiltration rates. Frequent freezing and thawing events in a soil may increase the soil erosion potential of a recently thawed soil [*Froese et al.*, 1999; *Ferrick and Gatto*, 2004]. Increases in air temperature should lead to enhanced soil temperatures, which is supported by observations of near-surface soil temperatures during winter and spring in the northern and northwestern United States from 1967 to 2002 [*Hu and Feng*, 2003]. An analysis of historical observations at several sites in the midwestern United States has found statistically significant increases in mean maximum and mean minimum winter soil temperatures leading to reductions in the annual number of soil frost days since 1966 [*Sinha et al.*, 2010]. However, during the winter season, soil temperature is directly influenced not

[1]School of Life Sciences, Arizona State University, Tempe, Arizona, USA.
[2]Department of Agricultural and Biological Engineering, Purdue Climate Change Research Center, Purdue University, West Lafayette, Indiana, USA.

0148-0227/10/2009JD012188

Table 1. SRES Scenarios[a]

Scenario	Description
B1	Describes a convergent world with global population that peaks in midcentury and declines thereafter. It describes rapid changes in economic structures toward service and information economy with introduction of clean and resources-efficient technologies with CO_2 concentrations stabilized at 550 ppm by the end of the century.
A1B	Describes a future world of very rapid economic growth, and the same global population pattern as B1, but with the rapid introduction of new and more efficient technologies. It is characterized by maximum CO_2 concentrations of 720 ppm.
A2	Describes a heterogeneous world with a gradual continuous increase in global population, regionally oriented economic growth and fragmented technological development. It reaches the maximum CO_2 concentration, 850 ppm by 2099, employed in this study and therefore experiences the maximum change in climate parameters.

[a]From *Nakicenovic et al.* [2000].

only by changes in air temperature but also by the timing and accumulation of snow [*Zhang et al.*, 2003]. Enhanced air temperatures are likely to result in reduced snowfall and shorter durations of snow on the ground which will further weaken the insulating effect of snow cover on the ground surface, potentially resulting in colder soil temperatures in the short term [*Hardy et al.*, 2001; *Sinha and Cherkauer*, 2008].

[4] Climate projections suggest that both air temperature and winter precipitation will increase by the end of the 21st century in the northern part of the Midwest [*Wuebbles and Hayhoe*, 2004]. This is likely to affect cold season processes and their interactions with other hydrologic variables such as runoff generation and soil moisture storage. The rise in soil temperature is likely to be enhanced in the future and may influence cold season hydrologic processes even more than changes in the recent past. Climate model projections indicate that the annual average daily maximum air temperature will increase from 2 to 9°C, winter precipitation will increase up to 30%, while summer precipitation may remain constant or decrease by the end of the 21st century [*Wuebbles and Hayhoe*, 2004]. Evaporation, runoff, and soil moisture are expected to increase throughout the region during the winter and spring months while the opposite will occur during summers. *Wuebbles and Hayhoe* [2004] also suggested that by 2090, the Midwest will experience an increase of 20 to 50 days annually when air temperatures exceed 32°C (i.e., a heat wave) as compared to the present climatic conditions. The annual number of days when air temperature falls below freezing is expected to decrease by 40 to 75 days by the end of 21st century. Several global climate models have used a scenario of $2 \times CO_2$ to suggest that the length of the thawed season will increase at low altitudes in the subarctic and the Arctic regions of North America while annual snowfall may or may not decrease [*Woo*, 1996].

[5] At river basin and global scales, several studies have examined the impact of projected future climatic change on hydrologic variables [e.g., *Christensen et al.*, 2004; *Barnett et al.*, 2005; *Milly et al.*, 2005; *Sheffield and Wood*, 2008], while fewer studies have focused on regional scales [e.g., *Hayhoe et al.*, 2004; *Wuebbles and Hayhoe*, 2004; *Cayan et al.*, 2008; *Adam et al.*, 2009; *Cherkauer and Sinha*, 2009]. The present study is different from other regional studies as it primarily focuses on future climate change impacts on the cold season processes of the midwestern United States. Cold season processes are not well represented at the grid resolution of global climate models, therefore, higher-resolution downscaled meteorological forcing data from climate models were used to drive the macroscale variable infiltration capacity (VIC) land surface model. The midwestern United States experiences variability in climate that affect flooding, the timing of frost and thaw, minimum soil temperatures, and soil moisture. Regional climatic changes are likely to result in changes to the spatial and temporal variability in cold season processes. Therefore, the objective of this study was to determine spatial and temporal patterns of cold season processes in response to future climate scenarios from 1977–2099. This work builds on previous studies conducted to understand historic climate variability effects on seasonal soil frost in the midwestern United States [*Sinha and Cherkauer*, 2008; *Sinha et al.*, 2010] through analysis of observations and retrospective model simulations.

2. Methods

[6] This study is focused on how future climate change affects cold season processes including those related to soil frost and snow cover in the midwestern United States. The impacts of future climate change were analyzed on various soil frost variables such as the number of soil frost days, the onset dates of soil freeze and thaw, and the number of freeze-thaw cycles. The following sections describe details concerning the future climate scenarios, meteorological forcing data set, the VIC model setup and evaluation, data processing, and climate sensitivity of cold season variables.

2.1. Future Climate Projections

[7] The projected climate data considered in this study were based on the climate models and scenarios used for the Intergovernmental Panel on Climate Change (IPCC) 4th Assessment Report (AR4) [*Meehl et al.*, 2007]. For this study, climate models were selected that: (1) have a varied range of spatial grid resolution (fine and coarse), (2) have the capability to represent realistic regional spatial structures of precipitation, and (3) have reasonable sensitivity to forcing by GHGs. Two global climate models were selected from the full set that met these criteria, one with the medium sensitivity, UK Met Office Hadley Center Climate Model, version 3.1 (HadCM3) [*Gordon et al.*, 2000; *Pope et al.*, 2000], and the other with high sensitivity to GHG forcing, National Oceanic and Atmospheric Administration (NOAA) Geophysical Fluid Dynamics Laboratory (GFDL) version CM2.1.1 [*Stouffer et al.*, 2006; *Delworth et al.*, 2006]. Three scenarios were selected from the Special Report on Emission Scenarios (SRES) [*Nakicenovic et al.*, 2000]; the B1,

Figure 1. Sites selected for the model evaluation: Waseca, MN (marked by the letter A) and Urbana, IL (marked by the letter B). Also shown is the climate sensitivity analysis of cold season processes representing (1) northwestern Minnesota, (2) northern Wisconsin, (3) southern Iowa, and (4) southern Indiana.

A1B, and A2 scenarios that describe different levels of population growth, economy, and energy consumption, which control their maximum atmospheric CO_2 concentrations (Table 1).

[8] Climate model projection data, for both models, and all three scenarios, came from the World Climate Research Programme's (WCRP's) Coupled Model Intercomparison Project phase 3 (CMIP3) multimodel data set, which was formally introduced by *Maurer et al.* [2007]. We made use of the Lawrence Livermore National Laboratory (LLNL)-Reclamation-Santa Clara University (SCU) downscaled climate projections derived from the WCRP's CMIP3 multimodel data set, stored and served at the LLNL Green Data Oasis. This data set was bias corrected using the method of *Wood et al.* [2004] before being used to drive the VIC model at a resolution of 1/8 degree latitude by longitude. Daily precipitation and air temperatures were developed from the monthly projections available from CMIP3 data set using the method outlined in the work of *Cherkauer and Sinha* [2009]. This involved classifying historic and future climate data into four climate categories (warm-wet, warm-dry, cool-wet and cool-dry), finding a climatically similar match between historic and future monthly data (e.g., a future February is classified as warm-wet so a warm-wet February was selected from the historic climatology), and then rescaling the daily time series by the change in monthly values between historic and future months. This results in a continuous daily time series that preserves the trends in precipitation and air temperature (maximum and minimum) from the GCMs, while also preserving the historic frequency of daily precipitation. The latter limitation of this method should not significantly affect the 30 year averages and cold season statistics used in the analysis.

2.2. VIC Model Setup and Evaluation

[9] Details of the VIC model are available in the work of *Liang et al.* [1994, 1996] and *Maurer et al.* [2002]. The soil and vegetation input parameters are described in the work of *Sinha et al.* [2010] but are summarized here for clarity. The VIC model version 4.1.0 r3 was used in this study with the finite difference thermal solution described by *Cherkauer and Lettenmaier* [1999] using a constant bottom boundary temperature based on the annual average air temperature for each grid cell. The initial temperature at the thermal damping depth of 10 m was set to average annual air temperature plus 5°C, to reflect the fact that soils that are seasonally frozen will remain warmer than the annual average air temperature. The model was allowed to spin up for 2 years, which has generally been found to be sufficient to reach thermal equilibrium or a state very close to it in regions of seasonal soil frost. To test this, the VIC model was spun up using periods of both 2 and 22 years resulting in differences of less than 2% in near-surface soil temperature and monthly frost depths for 98% of the total study area, while differences were within 5% for the remaining area during the overlap period of 1977–2006. Simulations were conducted on a 6 state region in the Midwest (MN, WI, MI, IA, IL, and IN). Soil parameters for the VIC model were obtained from *Mao and Cherkauer* [2009] and are based on the multilayer soil characteristics data set for the conterminous United States (CONUS-SOIL) [*Miller and White*, 1998] but regridded to a resolution of 1/8 degree latitude and longitude for three soil layers. A land-use map was developed at the VIC model resolution using vegetation classifications on the basis of 1 km resolution satellite data from 1992 to 1993 [*Hansen et al.*, 2000], with vegetation parameters taken from *Mao and Cherkauer* [2009].

[10] The model parameters were calibrated and evaluated using historic climate forcings, and regional observations of streamflow, and soil temperatures to obtain a single set of parameters over the 6 state study domain (details in the work of *Sinha et al.* [2010]). The calibrated model was then used in this study to predict soil temperatures, freeze-thaw depths, number of days with soil frost, and snow accumulation over the study region using the future climate forcings.

[11] Differences between the projected future climate (2010–2099) and current climate (1977–2006) were considered in studying how cold season hydrologic variables simulated by the VIC model have changed. By studying the differences, systematic biases were removed and the level of uncertainty owing to model parameterization was reduced. As the current and future simulations make use of the same soil and land use parameters, the analysis of simulated differences only accounted for changes due to the effects of climate variability.

2.3. Data Processing

[12] Annual statistics were computed for the time period starting from 1 September and ending on 31 August. This confined the entire cold season including the earliest onset of frost and last spring thaw within a single year. Cold season statistics were calculated for the period including winter and spring months (December–May) when most of the cold season processes such as snow accumulation and soil frost penetration were dominant in the study region. The dynamics outside of the cold season may play a role in the development of soil frost but such effects were not included in the current study. The following annual and cold season variables were estimated from the VIC model simulated

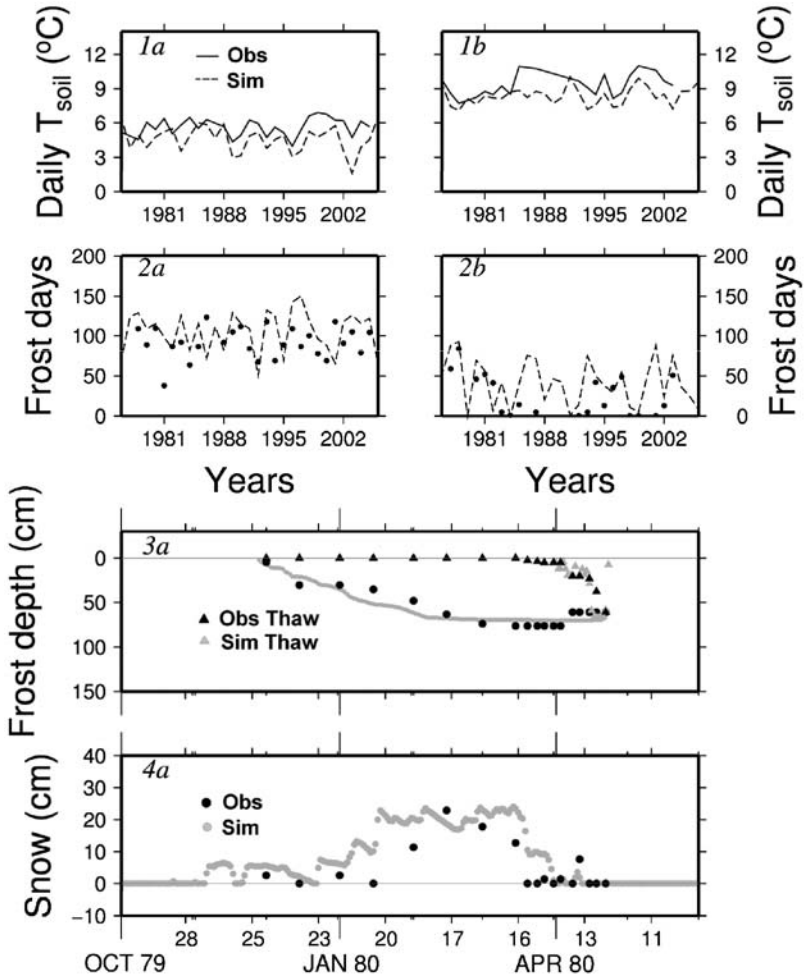

Figure 2. Sites selected for the model evaluation: Waseca, MN (scenarios 1a–4a) and Urbana, IL (scenarios 1b–2b) of cold season variables representing daily average soil temperature at 10 cm depth (scenarios 1a and 1b), average number of soil frost days at top 10 cm depth (cm) (scenarios 2a and 2b), average monthly frost depth (cm) (scenario 3a), and average monthly snow depth (cm) (scenario 4a).

daily time series of soil temperatures (T_{soil}) at a depth of 10 cm and gridded meteorological forcing data, using the methods described in the work of *Sinha and Cherkauer* [2008]:

[13] 1. Annual soil frost days computed by counting the number of days with frozen soil during a year. A temperature threshold of −0.25°C was defined to estimate soil frost days from the VIC model simulated extreme (maximum and minimum) daily soil temperatures. This is consistent with the analysis of *Sinha et al.* [2010], who found this threshold worked best in comparisons with observational data records.

[14] 2. Annual freeze-thaw cycles estimated by determining the number of times soil temperature changed between frozen and thawed states in a year.

[15] 3. Onset day of soil frost computed by calculating the first day since 1 September when soil was frozen.

[16] 4. Last thaw day computed by calculating the last day of soil frost since 1 September.

[17] 5. Days when average air temperature (T_{air}) < 0°C computed by calculating the number of days when daily average T_{air} (computed from daily minimum and maximum daily temperatures) was less than 0°C during a year.

Table 2. Description of Sites That Were Selected for Climate Sensitivity Analysis of Cold Season Variables

Site	Latitude	Longitude	Major Land Cover[a]	State	Average Cold Season T_{air} (°C)	Average Cold Season Precipitation (mm)
1	48.8125	−96.1875	grassland (0.5) and cropland (0.48)	MN	−5.4	150
2	46.0625	−91.0625	forest (0.92)	WI	−3.4	264
3	41.5625	−94.0625	cropland (0.55) and grassland (0.3)	IA	2.3	330
4	38.8125	−86.6875	forest (0.86)	IN	5.6	570

[a]Values in parentheses indicate fraction of land cover occupied in the single VIC grid cell.

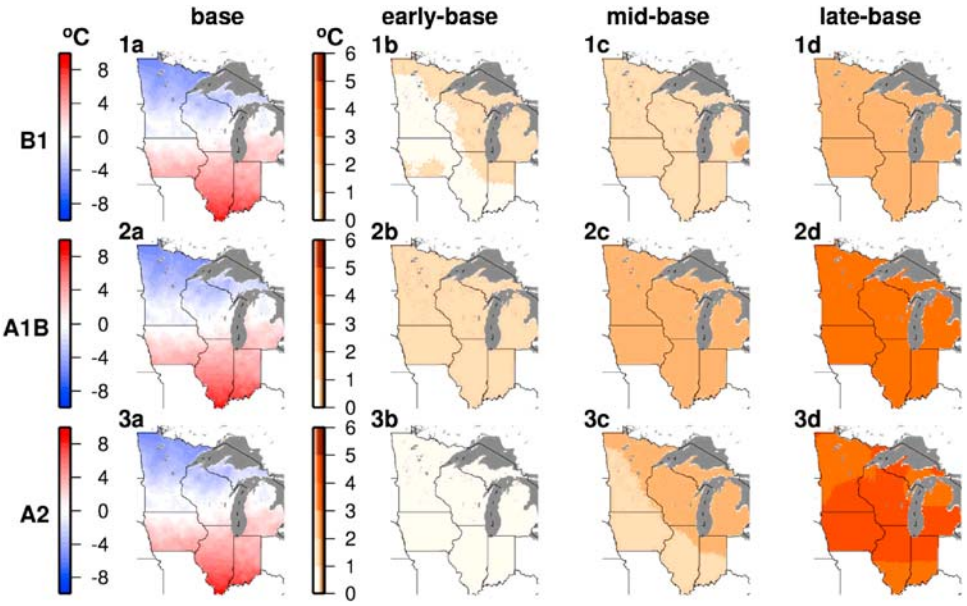

Figure 3. Downscaled air temperature change (°C) for the 21st century in early (2010–2039), middle (2040–2069), and late (2070–2099) century 30 year periods. Changes are relative to air temperatures during a base period of 1977–2006. Figures represent ensemble averages of the HadCM3 and GFDL climate model projections for B1 (scenarios 1a–1d), A1B (scenarios 2a–2d), and A2 (scenarios 3a–3d). All values are for the cold season (December through May).

[18] 6. Amount of snowfall computed from the daily meteorological data by calculating amount of precipitation when daily average air temperature was below 0°C for the cold season.

[19] 7. Average snow water equivalent (SWE) computed by averaging model simulated SWE for the cold season.

[20] 8. Average frost depth computed by averaging model simulated frost depth for the cold season.

[21] Ensemble averages were computed for the VIC simulated variables described above using both the GFDL and HadCM3 meteorological forcings for all three scenarios (B1, A1B, and A2). Changes in variables were calculated between the following 30 year groups: 1977–2006 (base), 2010–2039 (early century), 2040–2069 (midcentury), and 2070–2099 (late century). All discussions of change in variables were made with respect to the base period (1977–2006).

2.4. Model Evaluation

[22] Evaluation results for two of the sites used in the work of *Sinha et al.* [2010], Waseca, MN, and Urbana, IL, are presented in Figure 1. Comparison of daily average soil temperature and number of soil frost days at a depth of 10 cm indicate that the model captured the overall patterns observed at both sites (Figure 2, scenarios 1a–2b). Differences in absolute magnitudes were attributed to the use of grid cell average meteorological and soil data rather than data collected specifically at the observation site. The model simulations make use of 1/8 degree gridded meteorology data which was interpolated to the center of a grid cell using neighboring meteorological stations, which may affect the timing of precipitation, especially snowfall. In addition, the model used average soil conditions rather than site specific parameters, which influence soil moisture drainage, infiltration and heat conduction. Additionally, snow depth and frost depth simulations matched the observed data at Waseca site (MN) during the October to April season of 1979–1980 (Figure 2, scenarios 3a and 4a) (details described in the work of *Sinha et al.* [2010]). Overall, the VIC model was deemed acceptable to use as an analysis tool for analyzing future climate change impacts on cold season processes in the study domain.

2.5. Climate Sensitivity of Cold Season Variables

[23] Projections of future climate change indicated that the midwestern United States would experience increased air temperature and cold season precipitation. In order to study the sensitivity of cold season variables to climatic changes, the effects of increased air temperature and precipitation were analyzed at four sites under different climate and land use regimes using the VIC model (Figure 1).

Table 3. Downscaled Cold Season Air Temperature Change Relative to 1977–2006[a]

	Base	Change With Respect to Base		
Model	1977–2006 (deg C)	2010–2039 (deg C)	2040–2069 (deg C)	2070–2099 (deg C)
		GFDL		
B1	1.01	+1.06	+1.44	+1.90
A1B	0.94	+1.51	+2.24	+3.21
A2	1.06	+0.57	+1.70	+3.64
		HADCM3		
B1	0.70	+0.96	+2.04	+3.16
A1B	0.72	+1.98	+3.25	+4.23
A2	0.75	+0.82	+2.28	+4.47

[a]Cold season is defined as December–May.

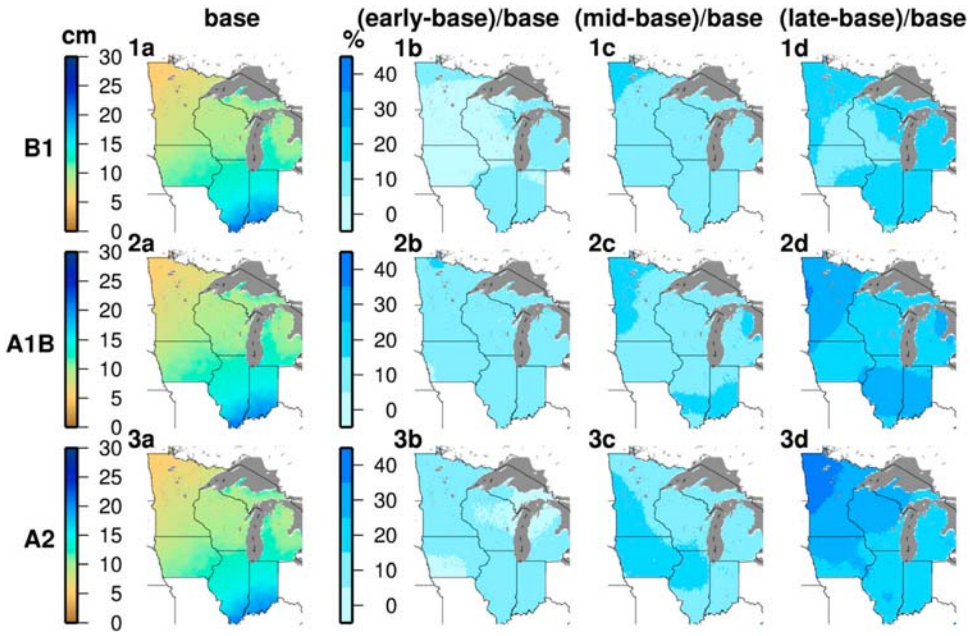

Figure 4. Downscaled precipitation change (percent) for the 21st century in early (2010–2039), middle (2040–2069), and late (2070–2099) century 30 year periods. Changes are relative to precipitation during a base period of 1977–2006. Figures represent ensemble averages of the HadCM3 and GFDL climate model projections for B1 (scenarios 1a–1d), A1B (scenarios 2a–2d), and A2 (scenarios 3a–3d). All values are for the cold season (December through May).

[24] The details of the sites are presented in Table 2. The VIC model simulations were performed at these sites from 1977 to 2006 under induced climatic conditions where daily average air temperature from the daily gridded meteorological data set was adjusted by ±2°C in increments of 1°C. Sensitivity to precipitation change was tested by running simulations with observed (1977 to 2006) precipitation, and with observed cold season precipitation increased by 30%. The five temperature and two precipitation scenarios resulted in ten simulations.

2.6. Analysis of Future Climate Projections

2.6.1. Air Temperature Projections

[25] Downscaled air temperature projections for the 6 state study region indicated that annual temperatures would increase by an average of about 4°C by the end of the century in comparison to the base period of 1977–2006. Of particular interest to this study were increases in the cold season air temperatures (December–May). Among all the scenarios, the increase in air temperature was highest for the late century period (2070–2099) (Table 3). During this period, the maximum projected increases in average seasonal air temperature across the study domain were 3.6°C and 4.5°C for the GFDL and HadCM3 A2 scenarios, respectively. The greatest change in air temperature occurred in the central part of the study domain (Figure 3, scenario 3d). In the late century period, both B1 and A1B scenarios indicated increases in air temperature throughout the region, though of lower magnitude than those projected by the A2 scenario (Figure 3, scenarios 1d and 2d). The A2 scenario, having the highest CO_2 concentrations among the selected SRES scenarios, resulted in the greatest change in air temperature by the late century period. However, in the early century period, the increase in air temperature was greater in the A1B scenario than in both the A2 and B1 scenarios, which experienced similar changes. In fact, the minimum changes in average air temperatures for both the GFDL and HadCM3 models (0.6°C and 0.8°C, respectively) were found for the A2 scenario in that early century period (Table 3 and Figure 3, scenario 3b).

2.6.2. Precipitation Projections

[26] All projected scenarios indicate that cold season precipitation was increasing for the study area (Table 4). The percentage increase in average precipitation varied from as low as 5% up to about 31% for the GFDL model, and from about 4% to 24% for the HadCM3 model (Table 4). Increases in average precipitation were highest for the late century period relative to the base period. Although the spatial patterns of average precipitation for the cold season varied during different time periods, all the scenarios projected an increase in the northern part of the study domain

Table 4. Downscaled Cold Season Precipitation Change Relative to 1977–2006[a]

	Base	Percent Change With Respect to Base		
Model	1977–2006 (mm)	2010–2039 (%)	2040–2069 (%)	2070–2099 (%)
		GFDL		
B1	332.3	+6	+9	+25
A1B	332.8	+10	+15	+31
A2	337.2	+5	+16	+28
		HADCM3		
B1	335.7	+4	+10	+10
A1B	339.3	+7	+11	+19
A2	326.6	+8	+12	+24

[a]Cold season is defined as December–May.

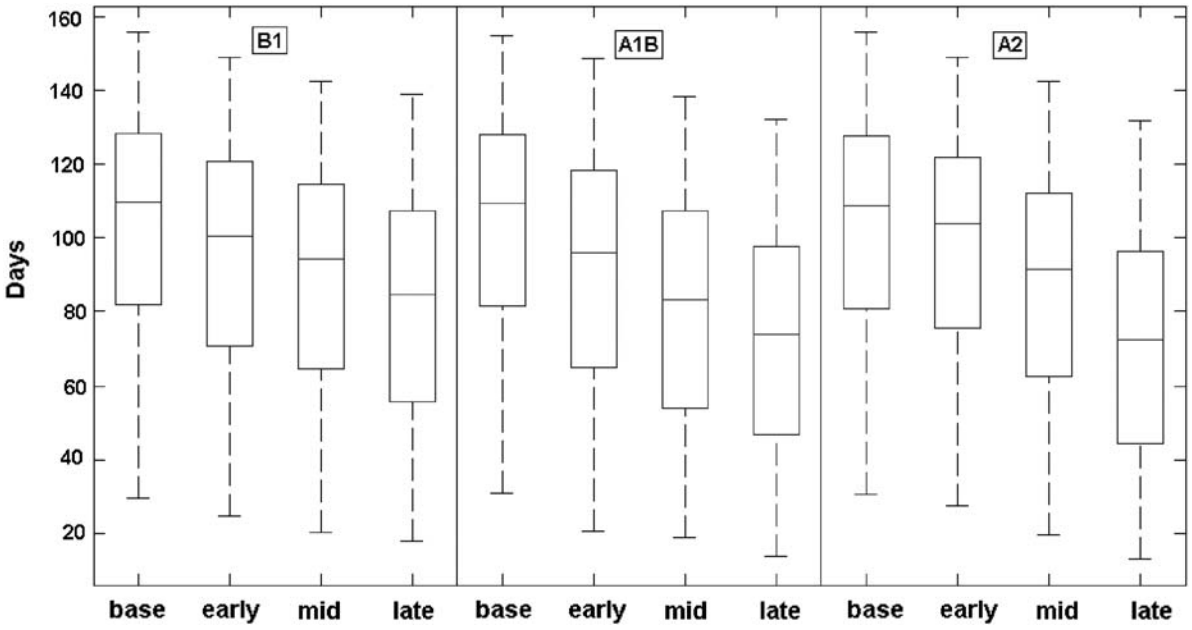

Figure 5. Box plots illustrate the distribution of the number of days when air temperature was less than 0°C for the B1, A1B, and A2 scenarios. Distributions are based on an ensemble of the HadCM3 and GFDL models for the following time periods: base (1977–2006), early century (2010–2039), midcentury (2040–2069), and late century (2070–2099). The lower tail of the box represents the minimum value, whereas the upper tail represents the maximum value of a series. The horizontal line represents the median, the lower edge of the box represents the 25th quartile, and the upper edge of the box represents the 75th quartile.

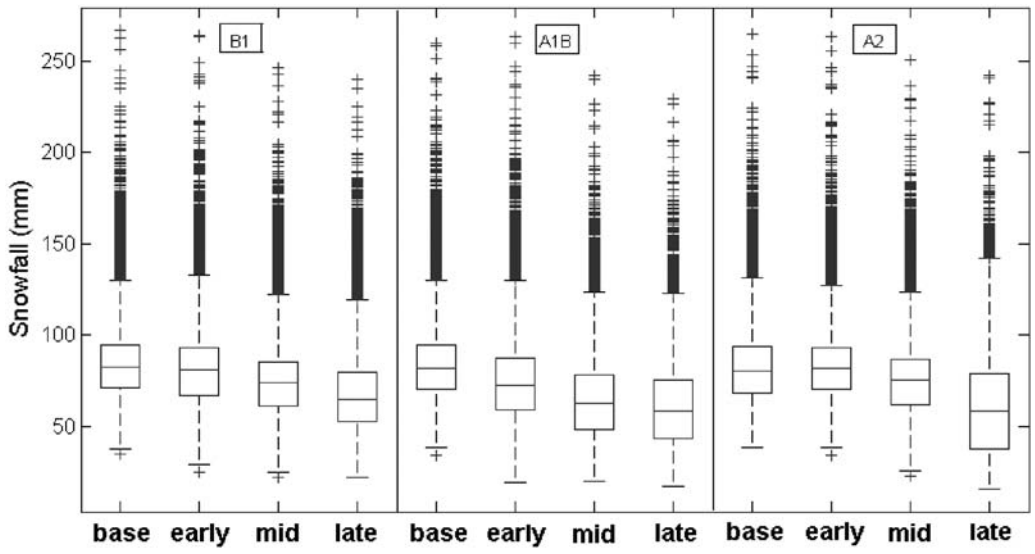

Figure 6. Box plots illustrate the distribution of amount of snowfall during the cold season for B1, A1B, and A2 scenarios. Distributions are based on an ensemble of the HadCM3 and GFDL models for the following time periods: base (1977–2006), early century (2010–2039), midcentury (2040–2069), and late century (2070–2099). Crosses indicate values that fell outside of 1.5 times the interquartile range and were therefore classified as outliers. Excluding outliers, the lower tail of the box represents the minimum value, whereas the upper tail represents the maximum value of a series. The horizontal line represents the median, the lower edge of the box represents the 25th quartile, and the upper edge of the box represents the 75th quartile.

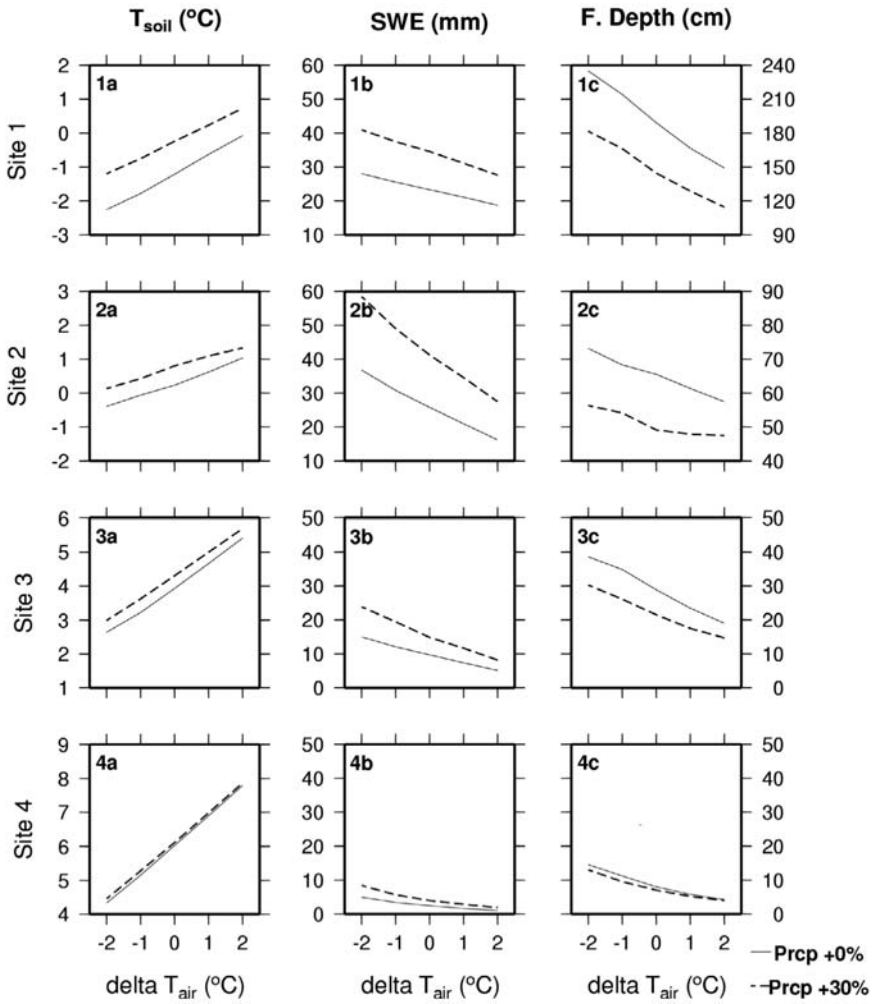

Figure 7. Climate sensitivity of the following selected cold season (December through May) variables: T_{soil}, soil temperature at a depth of 10 cm (°C) (scenarios 1a–4a); SWE, snow water equivalent (mm) (scenarios 1b–4b); and F. Depth, frost depth (cm) for four climate sensitivity sites (Figure 1) (scenarios 1c–4c). Delta T_{air} represents change in average daily air temperature, and Prcp represents change in daily precipitation (percent) relative to the gridded meteorology from 1977 to 2006.

(Figure 4). In addition, both the B1 and A1B scenarios experienced increased precipitation in the southern part of the study region during the late century period.

2.6.3. Below Freezing Air Temperature and Snowfall Projections

[27] The daily gridded meteorological forcings for each grid cell in the study domain was used to estimate annual days with below freezing T_{air} and cold season snowfall. These variables were estimated separately for both HadCM3 and GFDL models and then were averaged over the 30 year periods (base, early, middle, and late century) to determine their distribution for all grid cells. The median number of days when average $T_{air} < 0$°C decreased during the late century period in comparison to the base scenario by 25 days, 35 days, and 38 days for the B1, A1B, and A2 scenarios, respectively (Figure 5). Reductions were also projected in both the minimum and maximum (extreme) numbers of days with below freezing air temperatures. A similar decrease was observed in cold season snowfall for all the scenarios in the late century as compared to the base period, with higher reductions during the middle and late century periods (Figure 6). Median snowfall varied from 82 mm under the base period to 58 mm in both the A1B and A2 scenarios and 65 mm in the B1 scenario during the late century period. Although there was an increase in total precipitation (rain and snow), the amount of snowfall during the cold season decreased in the late century period with respect to the base period owing to increased air temperatures. Projected decreases in snowfall and enhanced air temperatures may result in lower snow accumulation that may leave the soil surface more exposed to fluctuations of air temperature during the cold season.

3. Results and Discussions

3.1. Sensitivity Analysis

[28] The sensitivity of six simulated variables to changes in air temperature and precipitation are shown in Figures 7 and 8. Increases in the average air temperature led to increased soil temperatures (T_{soil}), decreased snow water

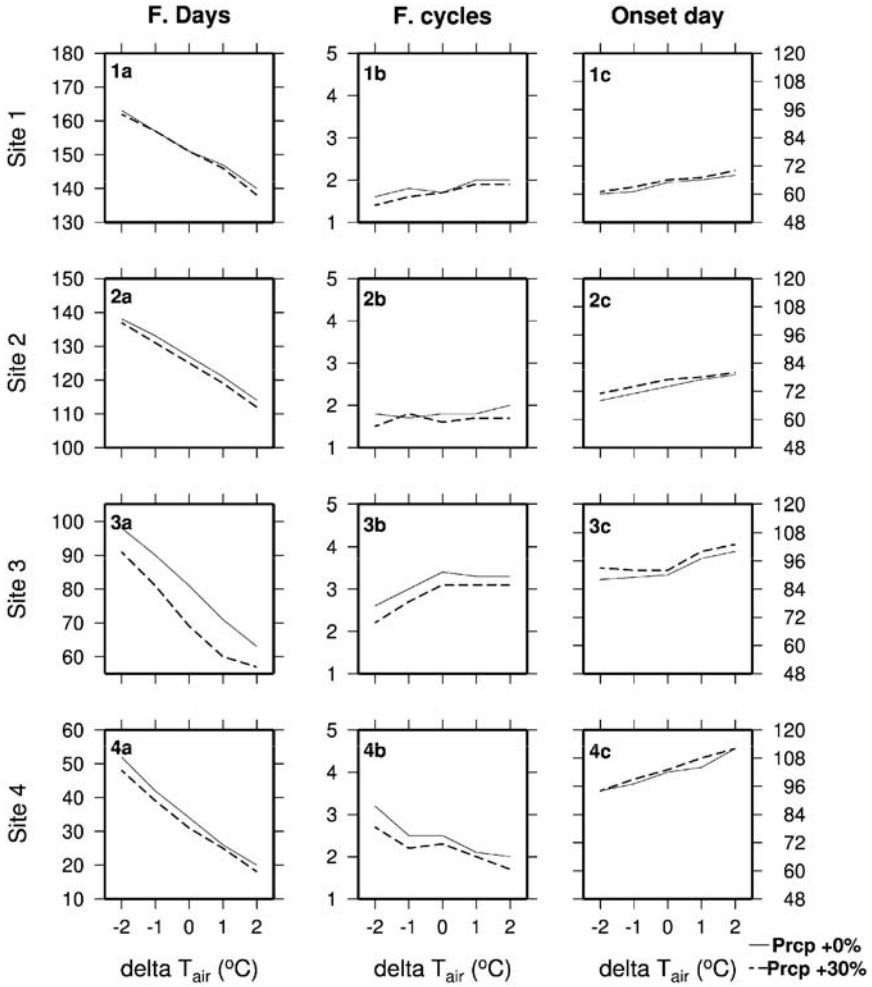

Figure 8. Climate sensitivity of the following selected cold season (December through May) variables: F. Days, frost days (number) (scenarios 1a–4a); F. cycles, freeze-thaw cycles (number) (scenarios 1b–4b); and Onset day, onset of first soil frost since 1 September for four climate sensitivity sites (Figure 1) (scenarios 1c–4c). Delta T_{air} represents change in average daily air temperature, and Prcp represents change in daily precipitation (percent) relative to the gridded meteorology from 1977 to 2006.

equivalents (SWE), and reduced frost depths at all four sites (Figure 7), as expected. Interestingly, the slopes of change in T_{soil} due to changes in air temperature were higher at sites 3 and 4, indicating that soils at southern Iowa and Indiana are more sensitive to increases in air temperature. This implies that a unit increase in air temperature will warm soils more at the southern sites than at the northern sites, which is likely related to the limited occurrence of soil ice in southern regions during the base period. With less energy devoted to phase change in the soil, more energy was available to change soil temperatures in comparison to northern regions.

[29] Increased precipitation led to changes in soil moisture and snow cover conditions which increased T_{soil} and SWE while reduced frost depth (Figure 7). Changes due to increased precipitation were greater at both the northern sites (Sites 1 and 2) than the southern sites. At the northern sites, the 30% increase in precipitation resulted in higher snowfall and an increased potential for snow accumulation even when temperatures increased above their current levels (Figure 7, scenarios 1b and 2b). Greater snow accumulation further insulated the ground from the subfreezing air temperatures of the northern regions, resulting in increased soil temperatures and decreased penetration of soil frost (Figure 7, scenarios 1c and 2c). Whereas, at the southern sites, similar changes in precipitation and air temperatures did not have as dramatic effect, leading to little to no change in the simulated variables (Figure 7, scenarios 3b–4c).

[30] However, changes in derived cold season variables, such as the number of days with soil frost, were found to be the same or larger for the southern sites than for the northern sites (Figure 8). These cold season variables were estimated from daily minimum and maximum T_{soil}, and were, therefore, more sensitive at the southern sites where T_{soil} changed most significantly. Increased precipitation did not have a significant effect on the number of soil frost days, freeze-thaw cycles or on the onset day of soil frost (Figure 8). For northern site 1, the average monthly near-surface T_{soil} changed from (−2.2°C to −1.2°C) when the air temperature was decreased by 2°C (at delta T_{air} = −2°C) while precipi-

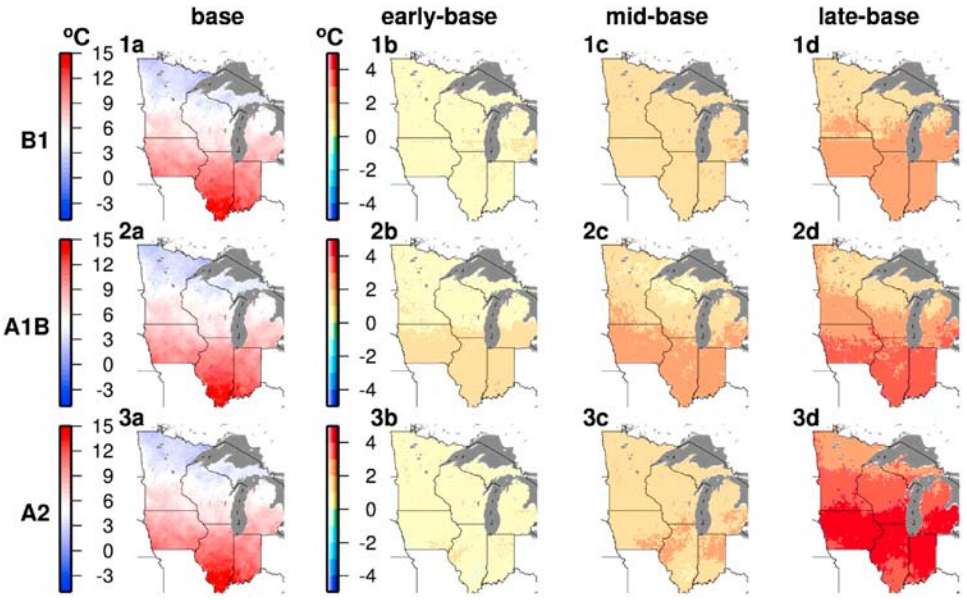

Figure 9. Soil temperature change (°C) for the 21st century in early (2010–2039), middle (2040–2069), and late (2070–2099) century 30 year periods. Changes are relative to soil temperatures during a base period of 1977–2006. Figures represent ensemble averages of the HadCM3 and GFDL climate model projections for B1 (scenarios 1a–1d), A1B (scenarios 2a–2d), and A2 (scenarios 3a–3d). All values are for the cold season (December through May).

tation increased by 30% from the base conditions (Figure 7, scenarios 1a and 2a). Although increased precipitation has led to an increase in near-surface T_{soil} by 1°C (and also decreased frost depth) by changing soil moisture and snow cover conditions, the near-surface daily minimum T_{soil} was still below freezing. Furthermore, Figure 7 (scenarios 1a–4a) only indicated monthly average near-surface soil temperatures but not the daily temperatures. Since the daily minimum soil temperatures were below subfreezing at the northern sites, the decrease in number of soil frost days were of the order of 2–3 days. In contrast, at southern sites 3 and 4, the near-surface soil temperatures increased well above 0°

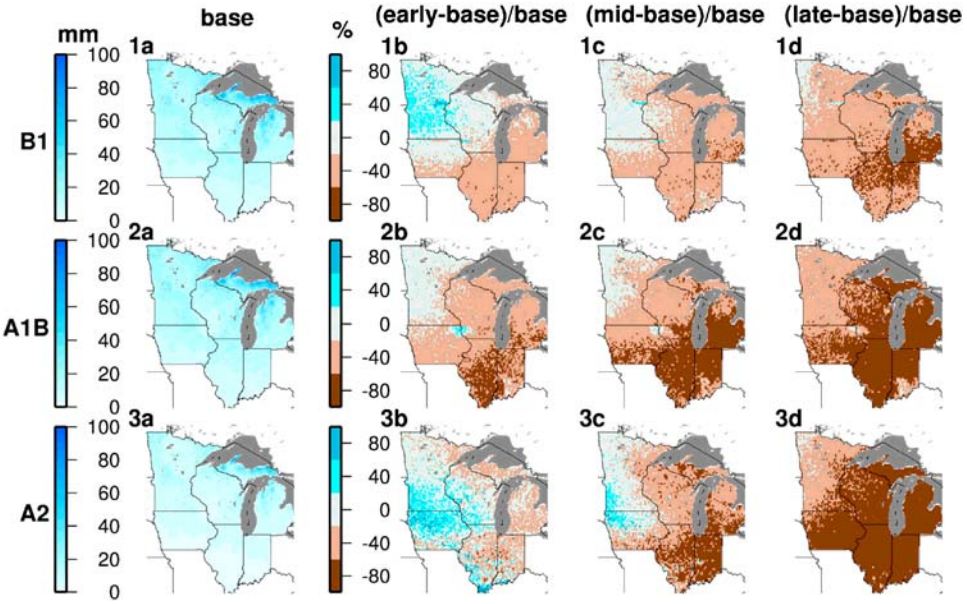

Figure 10. Snow water equivalent (SWE) change (percent) for the 21st century in early (2010–2039), middle (2040–2069), and late (2070–2099) century 30 year periods. Changes are relative to SWE during a base period of 1977–2006. Figures represent ensemble averages of the HadCM3 and GFDL climate model projections for B1 (scenarios 1a–1d), A1B (scenarios 2a–2d), and A2 (scenarios 3a–3d). All values are for the cold season (December through May).

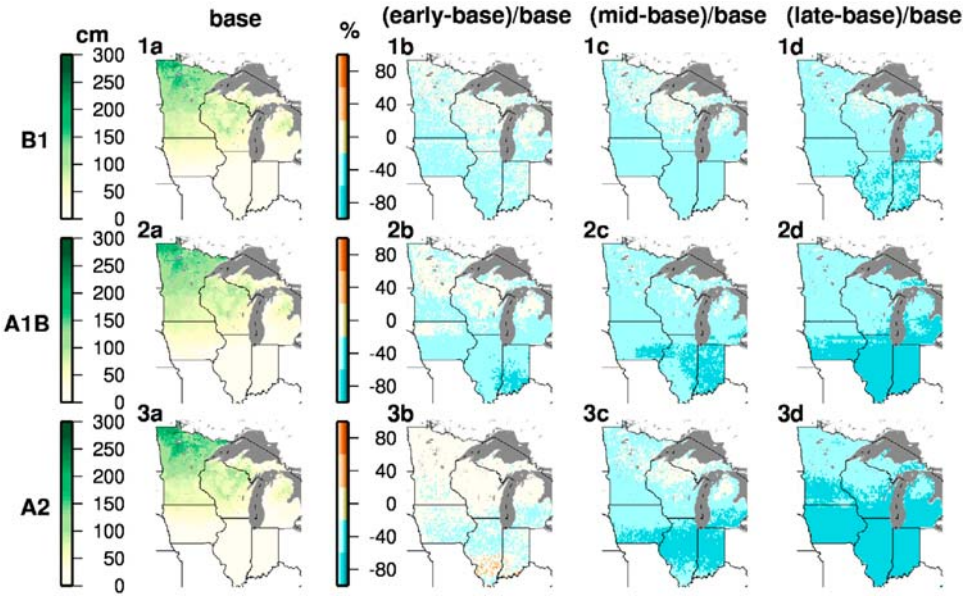

Figure 11. Frost depth change (percent) for the 21st century in early (2010–2039), middle (2040–2069), and late (2070–2099) century 30 year periods. Changes are relative to frost depth during a base period of 1977–2006. Figures represent ensemble averages of the HadCM3 and GFDL climate model projections for B1 (scenarios 1a–1d), A1B (scenarios 2a–2d), and A2 (scenarios 3a–3d). All values are for the cold season (December through May).

C, causing changes in soil frost days due changes in soil moisture conditions driven by increased precipitation.

3.2. Climate Change Scenarios Analysis

[31] In the case of the B1 scenario, changes in soil temperature during the early century period were found to be similar to those of air temperature, whereas in the late century period, T_{soil} increased up to 3°C in the southern regions with respect to the base scenario (Figures 3 and 9, scenarios 1b–1d). Southern regions also indicated higher reductions in SWE by about 50% from the base period SWE during middle and late century periods (Figure 10, scenarios 1c–1d). This reduction occurred despite a 20% increase in cold season precipitation (Figure 4, scenarios 1c–1d), and therefore, was likely due to increased air temperatures that reduced snowfall amounts. The change in the median cold season snowfall from 82 mm in the base period to 65 mm in the late century period indicated reductions in snowfall and the potential for reduced snow accumulations (Figure 6). In both the A1B and A2 scenarios, increased soil temperatures in the southern regions were greater than those for the B1 scenario by the late century period (Figure 9, scenarios 2d and 3d). This may be due to higher increases in air temperatures during the late century period under both A1B and A2 scenarios (Figure 3, scenarios 2d and 3d). Furthermore, sensitivity analysis of the four sites also indicated that soil temperatures at the southern sites were more susceptible to increases in air temperature than in the north.

[32] Interestingly, southern regions experienced reductions in SWE during the early century period for all three scenarios in comparison to the base period (Figure 10, scenarios 1b–3b). These reductions were greater for the A1B scenario, which may have resulted in increased soil temperatures in the southern region despite the uniform increase (within 2°C) in air temperature throughout the entire region (see Figure 9, scenario 2b, and Figure 3, scenario 2b). In contrast, the early century period indicated increased SWE for the B1 scenario in Minnesota and northern Wisconsin as well as for the A2 scenario in southern Minnesota, southwestern Wisconsin, and most of Iowa (Figure 10). The early century period experienced a similar increase in the amount of snowfall in both the B1 and A2 scenarios, in comparison to the base period (Figure 6). This may have resulted in similar or higher snow accumulations in these regions, leading to uniform or narrow range of changes (with 2°C) in soil temperatures throughout the region (Figure 9, scenarios 1b and 3b). Furthermore, sensitivity analysis indicated that at northern Minnesota and Wisconsin sites, increased precipitation resulted in higher SWE while increased air temperature decreased SWE (Figure 7, scenarios 1c and 2c), but changes in both minimized the individual effect of each on overall SWE levels. The overall effect of this change was less reduction in SWE in northern Minnesota during the late century period with respect to the base period (Figure 10, scenarios 1d–3d).

[33] In the late 21st century, frost depths were reduced, mostly in the central and southern regions in all the three scenarios (Figure 11, scenarios 1d–3d). The VIC model simulations indicate that on a monthly basis, the spatial average of soil frost penetration in the region during the base period was about 54 cm from the ground surface. The greatest change in average monthly soil depth penetration over the late century period was observed in the A2 scenario, where the frost depth changed to 22 cm. Furthermore, in the northern Minnesota (north of 46.5° latitude), monthly average frost depth changed from 137 cm to 77 cm during the late century period under the A2 scenario with respect to the base period. Similarly, during the same time period under the A2

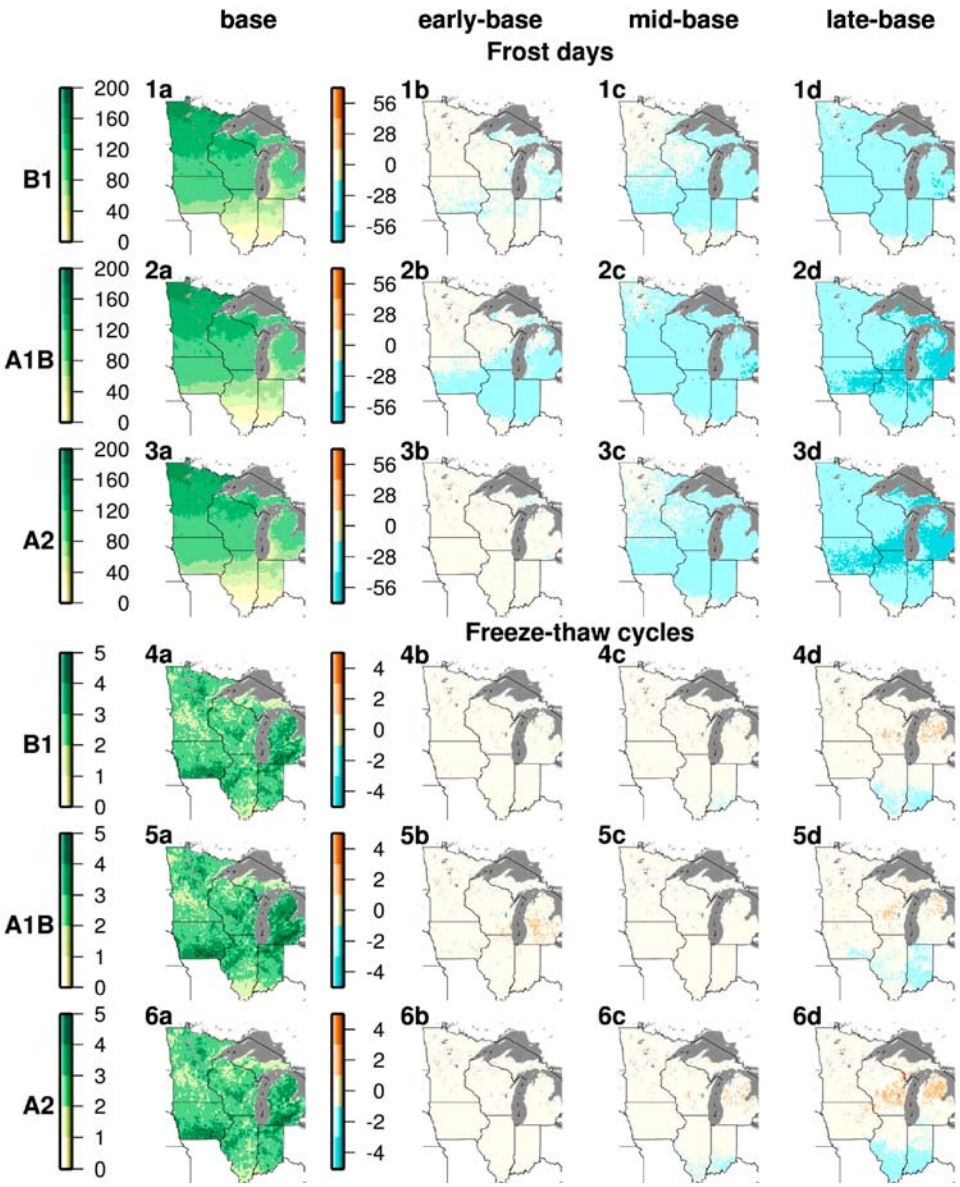

Figure 12. Changes in average number of soil frost days (numbers) and freeze-thaw cycles (numbers) for the 21st century in early (2010–2039), middle (2040–2069), and late (2070–2099) century 30 year periods. Changes are relative to soil frost days and freeze-thaw cycles during a base period of 1977–2006. Figures represent ensemble averages of the HadCM3 and GFDL climate model projections for the B1, A1B, and A2 scenarios.

scenario, average soil frost depth changed from 66 cm to 26 cm in central Wisconsin (between ~43.75° N and ~44.0° N latitude) and from 12 cm to less than 1 cm in central Indiana (between ~39.0°N to ~40.5°N latitude). Interestingly, the late century period reductions in SWE by 80% of the base conditions for the A2 scenario coincided with a reduction in the frost depth by similar percentage with respect to the base conditions in the southern study area (Figure 10, scenario 3d). SWE was reduced owing to decreased cold season snowfall and enhanced air temperatures that restricted snow accumulations by the late century period. Although we might expect an increase in soil frost penetration depth with decreased snow cover, increases in air temperature counteracted this change and hence resulted in shallower penetration of soil frost as indicated by reduced frost depth during the late century period.

[34] All climate scenarios indicated reductions in the annual number of soil frost days for middle and late century periods (Figure 12, scenarios 1c–3d). The reduction in soil frost days was about 45 days on average in the central regions of the study domain for the A2 scenario during the late century period. Such reductions were indicative of warmer soils, which may have occurred owing to the combined effect of increased air temperatures and decreased SWE in the central and southern regions of the study area. The smaller change in the number of soil frost days in the southern Indiana and

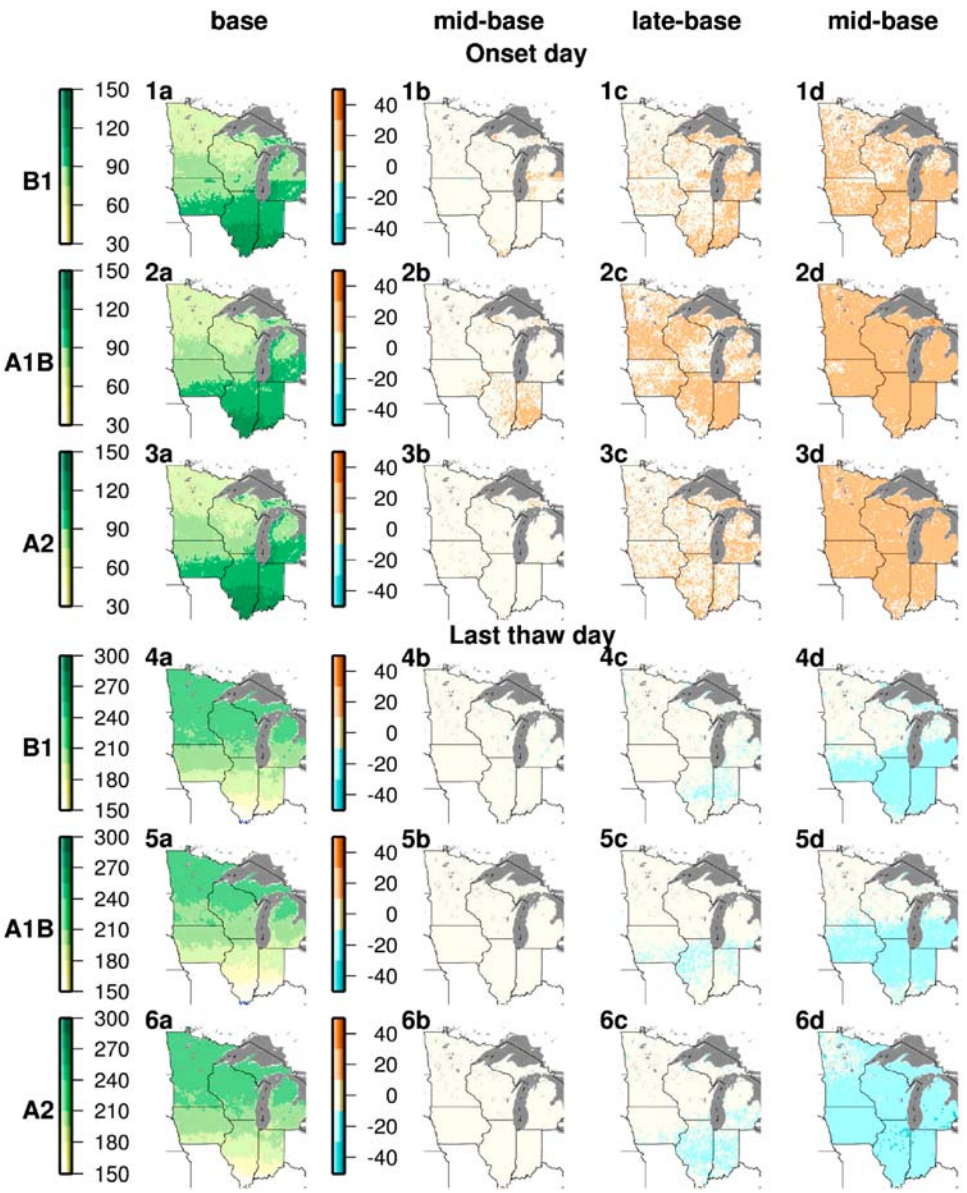

Figure 13. Changes in onset day of soil frost and last spring thaw for the 21st century in early (2010–2039), middle (2040–2069), and late (2070–2099) century 30 year periods. Changes are relative to onset day of soil frost and last spring thaw during a base period of 1977–2006. Figures represent ensemble averages of the HadCM3 and GFDL climate model projections for the B1, A1B, and A2 scenarios.

Illinois was a result of fewer days with soil frost in the current (base) conditions, so those areas were largely frost free by the end of the 21st century.

[35] The number of freeze-thaw cycles increased in south-central Wisconsin and northern regions of lower Michigan during the late century period where fewer days of below freezing air temperatures and shorter durations of snow cover caused more fluctuations of temperatures around 0°C (Figure 12, scenarios 4d–6d). The maximum increase in the number of cycles was three cycles during the late century period for the A2 scenario. Projections of increased freeze-thaw cycles in the Midwest is consistent with the findings of E. Takle and D. Hofstrand (see http://www.agmrc.org/renewable_energy/climate_change/climate_change__impact_on_midwestern_agriculture.cfm#) based on International Panel on Climate Change 2007 4th Assessment Report and from the U.S. Climate Change Science Program Synthesis and Assessment Report of 2008. The higher number of freeze-thaw cycles would increase the risk of soil erosion in these areas by weakening soil structure. Southern Indiana and Illinois, however, experienced a reduction in freeze-thaw cycles by as many as three cycles in the late century period owing to a rise in soil temperatures which provided fewer opportunities for freeze-thaw cycles to occur.

[36] The onset day of soil frost shifted later in the year for all scenarios, up to a maximum of 27 days for the late century period (Figure 13, scenarios 1d–3d). For the same time period, the last spring thaw occurred earlier in the study domain, but changes were most dramatic in the southern regions for the B1 and A1B scenarios, and throughout the

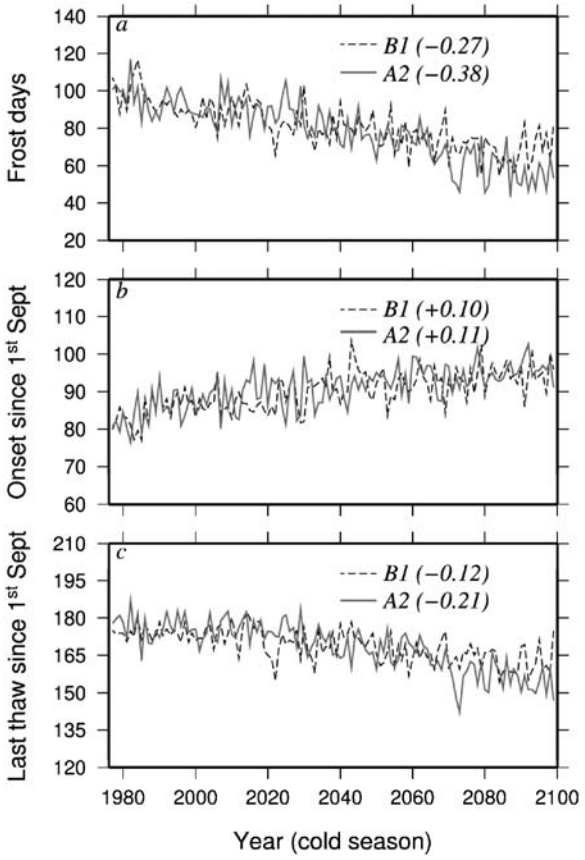

Figure 14. Time series of spatially averaged cold season variables: (a) number of soil frost days, (b) onset day of soil frost since 1 September, and (c) last thaw day of soil frost since 1 September for the B1 and A2 scenarios. The values in parentheses indicate Mann-Kendall's slope.

region for the A2 scenario (Figure 13, scenarios 4d–6d). The change in the date of last spring thaw was by as much as by 30 days earlier in most regions of Illinois and Indiana, and the southern regions of Iowa and lower peninsula Michigan. Therefore, the length of the soil frost season decreased by up to about two months under the A2 scenario during the late century period, but only from two to five weeks under the B1 scenario.

[37] A time series of spatially averaged variables for the study domain from 1977 to 2099 indicated a significant decrease in the number of soil frost days for both the B1 and A2 scenarios (Figure 14). The rate of decrease was highest for the A2 scenario (−0.38), which also experienced the greatest warming, but the most significant difference occurred after 2065 when the number of soil frost days dropped appreciably under the A2 scenario as compared to the B1 scenario. A similar reduction in the last thaw date of soil frost was observed after 2065 under the A2 scenario (−0.21) with respect to the B1 scenario (−0.12) (Figure 14c). Trends in the date of soil frost onset are similar between the A2 and B1 scenarios, with onset dates shifting almost 15 days later in the year between 1977 and 2099.

[38] Reductions in soil frost duration, especially in the date of last soil frost, have resulted in higher spring infiltration, but also greater drainage. This resulted in an 18% reduction of soil moisture in the top 10 cm soil layer for the late century period with respect to the base period (Figure 15). Specifically, the central regions of the study domain have experienced significant reductions in near-surface soil moisture. These regions also correspond to greater increases in near-surface soil temperatures (Figure 9) where crops could be planted earlier in spring resulting in a longer growing season. That could in turn increase ET in late spring drying soils further, something that is not represented by the VIC model as its vegetation parameters are fixed for each simulation. Although a potentially longer growing season may contribute to higher crop yields, it is also likely to increase the potential for invasion of pests owing to increased soil temperatures [*Simberloff*, 2000]. In the short term it is possible that lower snow accumulations will increase soil frost penetration as the soil is left without an insulating layer of snow [*Groffman et al.*, 2001; *Sinha and Cherkauer*, 2008]. Warmer air and increased precipitation may also increase the frequency of rainfall and snowmelt in the winter and spring, which could increase the likelihood of spring flooding if soil frost is present, such as occurred in northern Indiana during January and February 2008.

4. Conclusions

[39] In this study, future climate change impacts on cold season processes such as the number of soil frost days, snow accumulation, and soil temperatures were analyzed under three future climate scenarios using an ensemble of two CMIP3 model simulations in the midwestern United States. Downscaled and bias corrected global climate model forcing data were used to drive a macroscale land surface model to simulate selected soil frost and cold season variables. The response of those variables to future climate change was analyzed for four 30 year periods: 1977–2006 (base), 2010–2039 (early century), 2040–2069 (midcentury), and 2070–2099 (late century).

[40] The downscaled air temperature projections from the global climate simulations indicated an increase in air temperatures for the six states (MN, WI, MI, IA, IL, and IN) study area during the cold season (December through May). Specifically, the median number of days when air temperature was below 0°C reduced in the late century period in comparison to the base period by 25, 35, and 38 days for the B1, A1B, and A2 scenarios, respectively. This led to a decrease in median snowfall which varied from 82 mm under the base period to 58 mm in both the A1B and A2 scenarios and 65 mm in the B1 scenario during the late century period, despite an increase in total precipitation.

[41] All climate scenarios indicated reductions in the annual number of soil frost days, by about 45 days on an average in the A2 scenario during the late century period, mostly in the central regions of the study domain. This was indicative of increased soil temperatures owing to decreased SWE in the central and southern regions of the study area, where air temperatures were at or above 0°C. The number of freeze-thaw cycles increased in south-central Wisconsin and the northern regions of Michigan by up to three cycles per year. Increases in the frequency of freeze-thaw cycles may increase the risk of soil erosion in these areas. A delay of about 27 days was found in onset day of soil frost while the last spring thaw occurred by 30 days earlier in the worst case

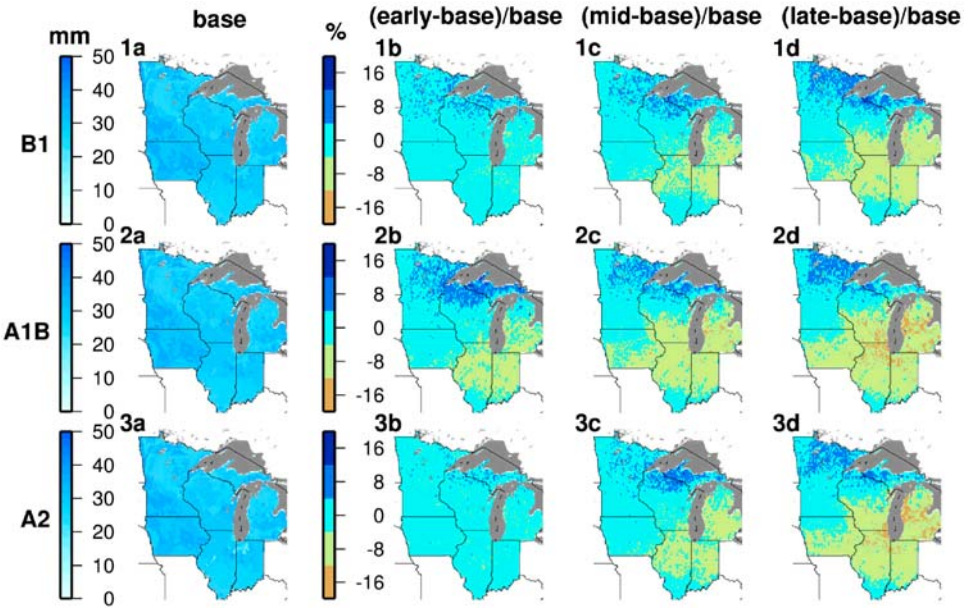

Figure 15. Near-surface soil moisture change (percent) in the top 10 cm layer for 21st century springs (March through May) in early (2010–2039), middle (2040–2069), and late (2070–2099) century 30 year periods. Changes are relative to soil moisture during a base period of 1977–2006. Figures represent ensemble averages of the HadCM3 and GFDL climate model projections for B1 (scenarios 1a–1d), A1B (scenarios 2a–2d), and A2 (scenarios 3a–3d).

scenario of A2 in the late century period. Therefore, the duration of the soil frost season decreased by up to two months in the A2 scenario by the end of the century.

[42] Longer growing seasons should provide favorable conditions during spring for planting, however, the projected rise in soil temperatures during the cold season is likely to increase the risk of pest infestation. Fewer days with soil frost implies higher infiltration, specifically during early spring which may result in decreased soil moisture retention and drier soils in spring owing to enhanced evapotranspiration losses as compared to the present (1977–2006) conditions. This may also reduce the risk of soil frost enhancing winter and spring flood events; however, increased precipitation in the winter months is likely to keep river levels higher throughout the cold season.

[43] **Acknowledgments.** We acknowledge the modeling groups, the Program for Climate Model Diagnosis and Intercomparison, and the WCRP's Working Group on Coupled Modeling for their roles in making available the WCRP CMIP3 multimodel data set. Support of this data set is provided by the Office of Science, U.S. Department of Energy. We thank NASA for providing funding for this research through the grant NNG04GP13P.

References

Adam, J. C., A. F. Hamlet, and D. P. Lettenmaier (2009), Implications of global climate change for snowmelt hydrology in the twenty-first century, *Hydrol. Processes*, *23*, 962–972.

Barnett, T. P., J. C. Adam, and D. P. Lettenmaier (2005), Potential impacts of a warming climate on water availability in snow-dominated regions, *Nature*, *438*, 303–309, doi:10.1038/nature04141.

Cayan, D. R., E. P. Maurer, M. D. Dettinger, M. Tyree, and K. Hayhoe (2008), Climate change scenarios for the California region, *Clim. Change*, *87*, suppl. 1, 21–42, doi:10.1007/s10584-007-9377-6.

Cherkauer, K. A., and D. P. Lettenmaier (1999), Hydrologic effects of frozen soils in the upper Mississippi River basin, *J. Geophys. Res.*, *104*, 19,599–19,610, doi:10.1029/1999JD900337.

Cherkauer, K. A., and T. Sinha (2009), Hydrologic impacts of projected future climate change in the Lake Michigan region, *J. Great Lakes Res.*, doi:10.1016/j.jglr.2009.11.012

Christensen, N. S., A. W. Wood, N. Voisin, D. P. Lettenmaier, and R. N. Palmer (2004), The effects of climate change on the hydrology and water resources of the Colorado River Basin, *Clim. Change*, *62*, 337–363, doi:10.1023/B:CLIM.0000013684.13621.1f.

Delworth, T. L., et al. (2006), GFDL's CM2 global coupled climate models—part 1: Formulation and simulation characteristics, *J. Clim.*, *19*, 643–674, doi:10.1175/JCLI3629.1.

Ferrick, M. G., and L. W. Gatto (2004), Quantifying the effect of a freeze-thaw cycle on soil erosion: Laboratory experiments, *Rep. ERDC/CRREL LR-04-16*, 47 pp., Eng. Res. and Dev. Cent., U.S. Army Corps of Eng., Washington, D. C.

Froese, J. C., M. C. Cruse, and M. Ghaffarzadeh (1999), Erosion mechanics of soils with an impermeable subsurface layer, *Soil Sci. Soc. Am. J.*, *3*, 1836–1841.

Gordon, C., C. Cooper, C. A. Senior, H. Banks, J. M. Gregory, T. C. Johns, J. F. B. Mitchell, and R. A. Wood (2000), The simulation of SST, seas ice extents and ocean heat transports in a version of the Hadley Center coupled model without flux adjustments, *Clim. Dyn.*, *16*, 147–168, doi:10.1007/s003820050010.

Groffman, P. M., C. T. Driscoll, T. J. Fahey, J. P. Hardy, R. D. Fitzhugh, and G. L. Tierney (2001), Effects of mild freezing on soil nitrogen and carbon dynamics in a northern hardwood forest, *Biochemistry*, *56*, 191–213.

Hansen, M. C., R. S. Defries, J. R. G. Townsheed, and R. Sohlberg (2000), Global land cover classification at 1 km spatial resolution using a classification tree approach, *Int. J. Remote Sens.*, *21*, 1331–1364, doi:10.1080/014311600210209.

Hardy, J. P., P. M. Groffman, R. D. Fitzhugh, K. S. Henry, A. T. Welman, J. D. Demers, T. J. Fahey, C. T. Driscoll, G. L. Tierney, and S. Nolan (2001), Snow depth manipulation and its influence on soil frost and water dynamics in a northern hardwood forest, *Biogeochemistry*, *56*, 151–174, doi:10.1023/A:1013036803050.

Hayhoe, K., et al. (2004), Emissions pathways, climate change, and impacts on California, *Proc. Natl. Acad. Sci. U. S. A.*, *101*, 12,422–12,427, doi:10.1073/pnas.0404500101.

Hu, Q., and S. Feng (2003), A daily temperature dataset and soil temperature climatology of the contiguous United States, *J. Appl. Meteorol.*, *42*, 1139–1156, doi:10.1175/1520-0450(2003)042<1139:ADSTDA>2.0.CO;2.

Intergovernmental Panel on Climate Change (IPCC) (2007), Summary for policymakers, in *Climate Change 2007: The Physical Science Basis, Contribution of Working Group I to the Fourth Assessment Report of the Intergovernmental Panel on Climate Change*, edited by S. Solomon et al., pp. 1–18, Cambridge Univ. Press, New York.

Kling, G. W., et al. (2003), *Confronting Climate Change in Great Lakes Regions: Impacts on Our Communities and Ecosystems*, 92 pp., Ecol. Soc. of Am., Union of Concerned Sci., Washington, D. C.

Lemke, P., et al. (2007), Observations: Changes in snow, ice and frozen ground, in *Climate Change 2007: The Physical Science Basis, Contribution of Working Group I to the Fourth Assessment Report of the Intergovernmental Panel on Climate Change*, edited by S. Solomon et al., pp. 337–383, Cambridge Univ. Press, New York.

Lettenmaier, D. P., A. W. Wood, R. N. Palmer, E. F. Wood, and E. Z. Stakhiv (1999), Water resources implications of global warming: A US regional perspective, *Clim. Change*, *43*, 537–579, doi:10.1023/A:1005448007910.

Liang, X., D. P. Lettenmaier, E. F. Wood, and S. J. Burges (1994), A simple hydrologically based model of land surface water and energy fluxes for general circulation models, *J. Geophys. Res.*, *99*, 14,415–14,428, doi:10.1029/94JD00483.

Liang, X., D. P. Lettenmaier, and E. F. Wood (1996), One-dimensional statistical dynamic representation of sub-grid spatial variability of precipitation in the two layer variable infiltration capacity model, *J. Geophys. Res.*, *101*, 21,403–21,422, doi:10.1029/96JD01448.

Mao, D., and K. A. Cherkauer (2009), Impacts of land-use change on hydrologic responses in the Great Lakes region, *J. Hydrol. Amsterdam*, *374*, 71–82, doi:10.1016/j.jhydrol.2009.06.016.

Maurer, E. P., A. W. Wood, J. C. Adam, D. P. Lettenmaier, and B. Nijssen (2002), A long-term hydrologically based dataset of land surface fluxes and states for the conterminous Unites States, *J. Clim.*, *15*, 3237–3251, doi:10.1175/1520-0442(2002)015<3237:ALTHBD>2.0.CO;2.

Maurer, E. P., L. Brekke, T. Pruitt, and P. B. Duffy (2007), Fine-resolution climate projections enhance regional climate change impact studies, *Eos Trans. AGU*, *88*(47), 504, doi:10.1029/2007EO470006.

Meehl, G. A., et al. (2007), Global climate projections, in *Climate Change 2007: The Physical Science Basis, Contribution of Working Group I to the Fourth Assessment Report of the Intergovernmental Panel on Climate Change*, edited by S. Solomon et al., pp. 747–843, Cambridge Univ. Press, New York.

Miller, D. A., and R. A. White (1998), A conterminous United States multilayer soil characteristics dataset for regional climate and hydrology modeling, *Earth Interact.*, *2*, 1–26, doi:10.1175/1087-3562(1998)002<0001:ACUSMS>2.3.CO;2.

Milly, P. C. D., K. A. Dunne, and A. V. Vecchia (2005), Global pattern of trends in streamflow and water availability in a changing climate, *Nature*, *438*, 347–350, doi:10.1038/nature04312.

Nakicenovic, N., et al. (2000), Summary for policymakers, in *Intergovernmental Panel on Climate Change Special Report on Emissions Scenarios*, edited by N. Nakicenovic and R. Swart, pp. 3–21, Cambridge Univ. Press, New York.

Pope, V. D., M. L. Gallani, P. R. Rowntree, and R. A. Stratton (2000), The impact of new physical parameterisations in the Hadley Center climate model—HadAM3, *Clim. Dyn.*, *16*, 123–146, doi:10.1007/s003820050009.

Santer, B. D., T. M. L. Wigley, T. P. Barnett, and E. Anyamba (1996), Detection of climate change and attribution of causes, in *Climate Change 1995: The IPCC Second Scientific Assessment*, edited by J. T. Houghton et al., pp. 407–444, Cambridge Univ. Press, New York.

Sheffield, J., and E. F. Wood (2008), Projected changes in drought occurrence under future global warming from multi-model, multi-scenario, IPCC AR4 simulations, *Clim. Dyn.*, *31*, 79–105, doi:10.1007/s00382-007-0340-z.

Simberloff, D. (2000), Global climate change and introduced species in United States forests, *Sci. Total Environ.*, *262*, 253–261, doi:10.1016/S0048-9697(00)00527-1.

Sinha, T., and K. A. Cherkauer (2008), Time series analysis of freeze and thaw processes in Indiana, *J. Hydrometeorol.*, *9*, 936–950, doi:10.1175/2008JHM934.1.

Sinha, T., K. A. Cherkauer, and V. Mishra (2010) Impacts of historic climate variability on seasonal soil frost in the midwestern United States, *J. Hydrometeorol.*, in press.

Stouffer, R. J., et al. (2006), GFDL's CM2 global coupled climate models—part 4: Idealized climate response, *J. Clim.*, *19*, 723–740, doi:10.1175/JCLI3632.1.

Woo, M. K. (1996), Hydrology of North America under global warming, in *Regional Hydrology Response to Climate Change*, edited by J. A. A. Jones et al., pp. 73–86, Kluwer Acad., Norwell, Mass.

Wood, A. W., L. R. Leung, V. Sridhar, and D. P. Lettemaier (2004), Hydrologic implications of dynamical and statistical approaches to downscaling climate model outputs, *Clim. Change*, *62*, 189–216, doi:10.1023/B:CLIM.0000013685.99609.9e.

Wuebbles, D. J., and K. Hayhoe (2004), Climate change projections for the United States Midwest, *Mitigation Adaptation Strategies Global Change*, *9*, 335–363, doi:10.1023/B:MITI.0000038843.73424.de.

Zhang, T., M. Serreze, R. G. Barry, D. Gilichinsky, and A. Etringer (2003), Climate change: Evidence from Russian historical soil temperature measurements, *Eos Trans. AGU*, *83*(47), Fall Meet. Suppl., Abstract U72A-0008.

K. A. Cherkauer, Department of Agricultural and Biological Engineering, Purdue Climate Change Research Center, Purdue University, 225 S. University St., West Lafayette, IN 47907-2093, USA.

T. Sinha, School of Life Sciences, Arizona State University, P. O. Box 874501, Tempe, AZ 85287-4501, USA. (tsinha4@asu.edu)